ACS OMEGA

http://pubs.acs.org/journal/acsodf

Article

Effect of Variations in the Alkyl Chain Lengths of Self-Assembled Monolayers on the Crystalline-Phase-Mediated Electrical Performance of Organic Field-Effect Transistors

Myeongjin Park, Chan-mo Kang, Sangwook Park, Hyeona Jo, and Jeongkyun Roh*

Cite This: *ACS Omega* 2021, 6, 33639−33644

Read Online

ACCESS | Metrics & More | Article Recommendations | Supporting Information

ABSTRACT: Self-assembled monolayers (SAMs) of organic molecules are frequently employed to improve the electrical performance of organic field-effect transistors (OFETs). However, the relationship between SAM properties and OFET performance has not been fully explored, leading to an incomplete understanding of the system. This study investigates the effect of the SAM alkyl chain length on the crystalline phase of pentacene films and OFET performance. Two types of SAMs—with alkyl chain lengths of 10 (decyltrichlorosilane, DTS) and 22 (docosyltrichlorosilane, DCTS)—were examined, and variations in the performance of pentacene-based OFETs with the nature of the SAM treatment were observed. Despite the similar surface morphologies of the pentacene films, field-effect mobility in the DCTS-treated OFET was twice that in the DTS-treated OFET. To find the reason underlying the dependence of the OFET's electrical performance on the SAM alkyl chain length, X-ray diffraction measurements were conducted, followed by a phase analysis of the pentacene films. Bulk and thin-film phases were observed to coexist in the pentacene film grown on DTS, indicating several structural defects in the film; this can help explain the dependence of the OFET electrical performance on the SAM alkyl chain length, mediated by the different crystalline phases of pentacene.

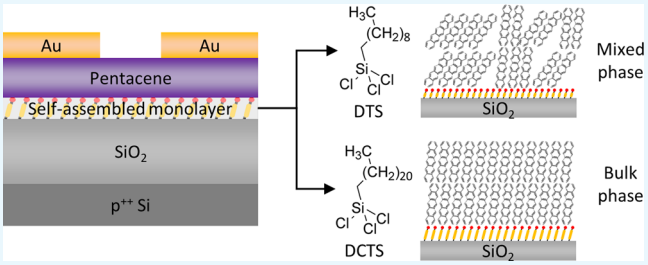

INTRODUCTION

Organic field-effect transistors (OFETs) have been attracting considerable attention due to their attractive features such as solution processability,[1,2] flexibility,[3,4] and availability for use in both p- and n-type semiconductors.[5] Intensive studies in the fields of material science and device engineering have led to significant improvements in their electrical performance, and as a result, their field-effect mobility (μ_{FET}) has surpassed that of amorphous silicon ($\mu_{FET} \sim 0.1$ cm V^{-1} s^{-1}) and is now comparable to that of oxide semiconductors ($\mu_{FET} > 10$ cm V^{-1} s^{-1}).[6,7] In addition to this remarkable progress in electrical performance, the expanding applications of OFETs in the neuromorphic computing of synaptic devices have garnered increasing levels of attention.[8,9]

Among several organic semiconductors, pentacene has played an important role in the development of OFETs as a material test platform. Due to its wide availability and decent electrical performance and stability, several theories—of contact resistance, bias stability, and threshold voltage control—have been developed on the device physics of pentacene-based OFETs.[10−12] Furthermore, initial demonstrations of various OFET applications, such as flexible electronic circuits, memory, and sensors, have involved the use of pentacene-based OFETs.[13−15] Although the mobilities of certain recently designed organic semiconductors are higher than that of pentacene, pentacene is still widely regarded as a standard material for p-type OFETs, with detailed investigations being conducted to explain the device performance of pentacene-based OFETs. Charge transport in pentacene, which directly determines the performance of its OFETs, is significantly influenced by the property of the semiconductor−dielectric interface.[16,17] The surface energy of the gate insulator significantly impacts the growth and packing density of the organic molecules, and interfacial trap states significantly hinder the efficient transport of carriers. To improve the performance of pentacene-based OFETs, various studies have been conducted to engineer the properties of the semiconductor−dielectric interface; the application of self-assembled monolayers (SAMs) to the gate insulator has been found to be one of the most effective approaches for this purpose.[18,19] Surface trap states at the interface can be effectively passivated by an anchoring group of the SAM, and simultaneously, the surface energy of the gate insulator is modified by a hydrophobic alkyl chain or functional group of the SAM.[20−23] As a result of this reduction in the number of

Received: August 19, 2021
Accepted: November 22, 2021
Published: November 30, 2021

interfacial trap states and/or the improvements in the semiconductor morphology arising from the SAM treatment, the OFET performance has dramatically increased in terms of field-effect mobility and bias stability.[24−26] However, despite the numerous reports on improvements in the OFET performance arising from the SAM treatment, the lack of detailed studies to examine the effect of SAM properties on device performance has led to an incomplete understanding of the system. Such studies need to be conducted to fully exploit the benefits of the SAM treatment to further improve the device performance.

In this study, we investigated the effects of the SAM alkyl chain length on the crystalline phase of pentacene films and OFET performance. We employed two types of trichlorosilane SAMs (with chain lengths of 10 and 22) and examined the electrical performance of the OFETs with and without the SAM treatment. The water contact angle and atomic force microscopy (AFM) measurements showed that both the varieties of SAMs effectively generated hydrophobic surfaces with similar water contact angles, consequently yielding pentacene thin films of similar morphologies. Despite this, however, the OFET performance varied significantly with the alkyl chain length of the SAM. To find the origin of this dependency, X-ray diffraction (XRD) measurements, followed by a crystalline phase analysis of pentacene films grown on each of the two SAMs, were conducted. The bulk phase was predominantly observed in the film grown on the longer SAM (with an alkyl chain length of 22), while the film grown on the shorter SAM (with an alkyl chain length of 10) exhibited a mixture of bulk and thin-film phases. As a result, shorter-SAM-treated OFETs have lower field-effect mobilities than longer-SAM-treated OFETs because of the structural traps in the pentacene film originating from the coexistence of two pentacene polymorphs. The finding of this work would enable a better and deeper understanding of the use of SAMs in OFET systems and, consequently, would help researchers and engineers fully exploit it for beneficial uses.

RESULTS AND DISCUSSION

Figure 1a shows the structure of pentacene-based OFETs treated with a trichlorosilane SAM. As shown in the figure, the SiO_2 surface is modified by both SAMs—decyltrichlorosilane (DTS) and docosyltrichlorosilane (DCTS). Both DTS and DCTS have similar chemical structures, except for the difference in their alkyl chain lengths: the former is 10 carbon atoms long, while the latter is 22 carbon atoms long, as shown in Figure 1b—the length of DCTS is about twice that of DTS. As the test SAM materials, we chose DTS and DCTS because trichlorosilane SAMs have rarely been employed when investigating the effect of SAM alkyl chain lengths on the OFET performance. Table S1 in the Supporting Information summarizes the previous studies that investigated the SAM-alkyl-chain-length-dependent performance of pentacene-based OFETs. As shown in the table, phosphonic-acid-based SAMs with various alkyl chain lengths have been frequently employed compared to the trichlorosilane-based SAMs. In order to provide a clue for understanding OFET systems with a trichlorosilane SAM treatment, we decided to employ two types of trichlorosilane SAMs with different alkyl chain lengths. We first determined the hydrophobicity of the SAM-treated SiO_2 surface using water contact angle measurements to check if the SAMs effectively modified the surface property of SiO_2. Figure 1c shows the water contact angles on pristine, DTS-treated, and DCTS-treated SiO_2 surfaces. The initially hydrophilic SiO_2 surface, with a water contact angle of 60°, becomes hydrophobic with larger contact angles of 107 and 105° after DTS and DCTS treatments, respectively. The high hydrophobicity of the SAM-treated surface is beneficial for the OFET fabrication because of the low surface trap density and the presence of more favorable surface states for better film growth. We measured the surface morphologies of pentacene films grown on pristine, DTS-treated, and DCTS-treated SiO_2. As shown in Figure 1d, the pentacene grown on SiO_2 exhibits a three-dimensional, island film growth with a nonuniform grain size. On the other hand, the pentacene films grown on DTS (Figure 1e) and DCTS (Figure 1f) were more tightly packed with uniform grain sizes, indicating the layered film growth on the SAM-treated SiO_2 surface. The charge transport of the layered film growth is better than that of the island-like film growth because of better interconnection between grains. From the similar AFM surface morphologies of pentacene on DTS and DCTS, it can be speculated that both the SAMs would cause comparable improvements in the electrical performance of the OFETs.

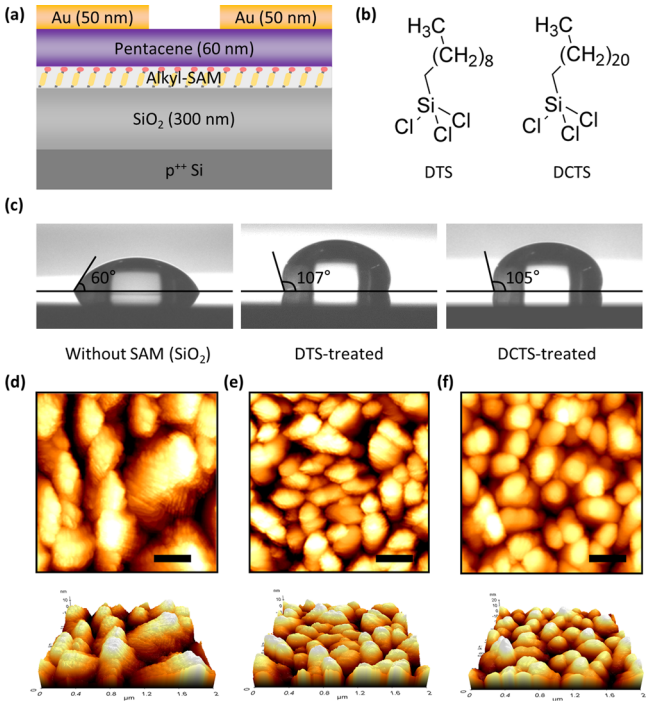

Figure 1. (a) Device structure of pentacene-based OFETs and (b) chemical structures of the trichlorosilane SAMs of different alkyl chain lengths used in this study. (c) Water contact angle measurements on pristine (left), DTS-treated (middle), and DCTS-treated (right) SiO_2 surfaces. 2D (top) and 3D (bottom) AFM images of the surface morphologies of the 60 nm pentacene films on (d) pristine, (e) DTS-treated, and (f) DCTS-treated SiO_2.

We then fabricated pentacene-based OFETs in the presence and absence of the SAM treatment and compared their electrical performances. Figure 2a shows the transfer characteristics of the OFETs with and without the SAM treatment, obtained in the saturation region where the drain-to-source voltage (V_{DS}) is −40 V. The field-effect mobility (μ_{FET}) and threshold voltage (V_{TH}) were extracted using the current−voltage equation in the saturation region

https://doi.org/10.1021/acsomega.1c04519
ACS Omega 2021, 6, 33639−33644

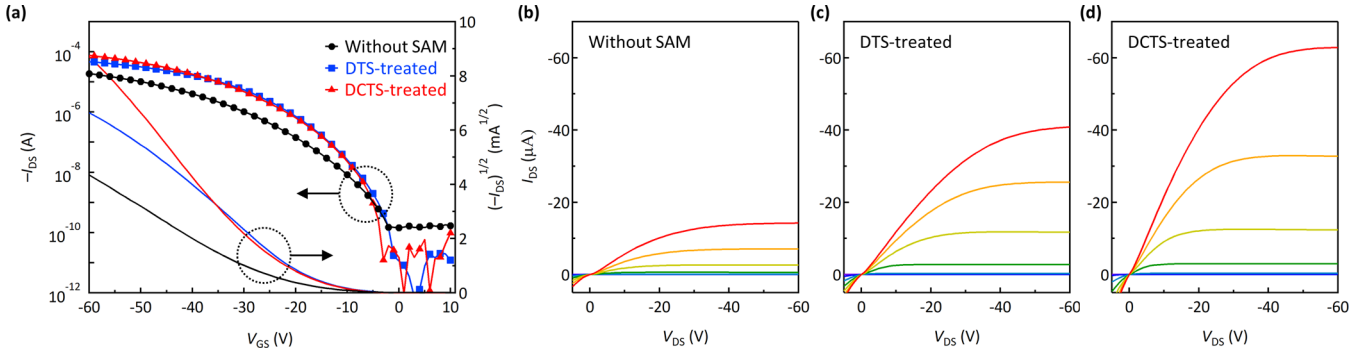

Figure 2. (a) Transfer characteristics of OFETs with and without the SAM treatment, measured in the saturation region with a drain-to-source voltage of −40 V. The output characteristic of the OFET (b) without the SAM treatment, (c) with the DTS treatment, and (d) with the DCTS treatment.

$$I_{DS} = \frac{1}{2}\mu_{FET}C_{ox}\frac{W}{L}(V_{GS} - V_{TH})^2 \quad (1)$$

where I_{DS} is the drain-to-source current, V_{GS} is the gate-to-source voltage, and C_{ox} is the unit capacitance of the gate insulator. The extracted field-effect mobility for the OFETs that underwent no SAM treatment was 0.10 cm^2 V^{-1} s^{-1}; this value increased to 0.20 and 0.39 cm^2 V^{-1} s^{-1} after DTS and DCTS treatments, respectively. Notable increases in the field-effect mobilities are also represented by the increase in the drain-to-source current in the output characteristics shown in Figure 2b–d. The improved performance of OFETs by interfacial engineering methods such as the SAM treatment is resulted from the combination of (i) an improved morphology of the organic semiconductor and (ii) a reduced energetic disorder in the organic semiconductor. It has been found that the former one is predominant in the case of polycrystalline materials and the latter one plays a more significant role in the case of amorphous materials. Because pentacene is a polycrystalline material, the major origin for the modified electrical performance by the SAM treatment should be ascribed to the different morphologies of pentacene films on SAMs. Therefore, in this study, we focus on the morphological effect. Nonetheless, it is still noting that the improved OFET performance by the SAM treatment is partially attributed to the reduced degree of the dipole-induced energetic disorder in the pentacene films.

The increase in the field-effect mobilities of the OFETs arising from their SAM treatment agrees with our speculation based on the AFM surface morphologies; the SAM treatment yielded a denser pentacene film, which was beneficial for charge transport. Since both the SAMs exhibit very similar surface morphologies, the 2-fold increase in the field-effect mobility of the DCTS-treated OFET relative to that of the DTS-treated OFET, however, cannot be explained solely by the AFM measurement results. The gap in the understanding of the effect of SAM properties on OFET electrical performance lies in determining the effect of its alkyl chain length on the OFET performance. To investigate this, we conducted XRD measurements on the pentacene films grown on pristine, DTS-treated, and DCTS-treated SiO_2 (Figure 3a). As shown in the diffraction patterns, a series of Bragg peaks corresponding to the (00l) planes appeared without any other (hkl) reflections for all pentacene thin films, indicating a fair orientation of the pentacene crystals in their (00l) planes, which was parallel to the SiO_2 surface. There exist two distinct Bragg peaks, each of which represents different pentacene

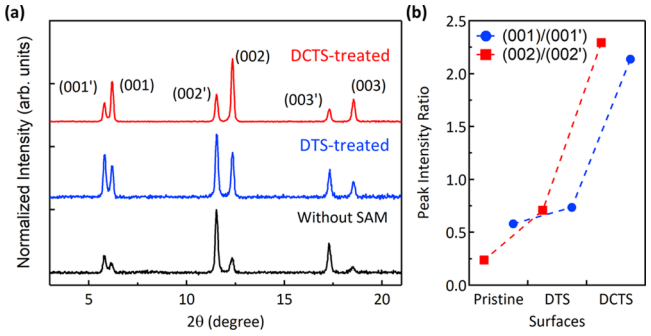

Figure 3. (a) XRD patterns of the 50 nm pentacene films on pristine, DTS-treated, and DCTS-treated SiO_2. (b) Peak intensity ratio (i.e., $I_{peak\_bulk}/I_{peak\_thin\ film}$) of the pentacene films on pristine, DTS-treated, and DCTS-treated SiO_2.

polymorphs; the peaks occur at 5.78 and 6.17° and the corresponding d_{001}-spacings of the pentacene films can be calculated from Bragg's law, which is depicted by the equation $n\lambda = 2d \sin\theta$, where n is the diffraction order, λ is the wavelength, d is the interplanar spacing, and θ is the incidence angle. The calculated d_{001}-spacings are 15.3 and 14.3 Å and correspond to the thin-film and bulk phases, respectively. The presence of two Bragg peaks implies a mixture of the two types of pentacene polymorphs in the films, but the fraction of each component varies with the underlying surfaces. For the quantitative analysis, we calculated the ratios of the peak intensity of the bulk phase (I_{peak_bulk}) to that of the thin-film phase ($I_{peak\_thin\ film}$) (Figure 3b). The pentacene film grown on the pristine SiO_2 surface displays thin-film phase dominancy (i.e., $I_{peak\_bulk}/I_{peak\_thin\ film} \ll 1$) while that on DCTS exhibits a bulk phase dominancy (i.e., $I_{peak\_bulk}/I_{peak\_thin\ film} \gg 1$). The pentacene film on DTS is dominated by neither phase; instead, both phases coexist in the film, producing a mixed phase (i.e., $I_{peak\_bulk}/I_{peak\_thin\ film} \sim 0.7$). Using these observations, the growth of pentacene thin films on each surface can be schematically illustrated, as shown in Figure 4. As shown in Figure 4a, the thin-film phase is predominant in the pentacene grown on the pristine SiO_2 surface. The thin-film phase is known to be beneficial for efficient charge transport,[27,28] but the hydrophilic SiO_2 surface results in a three-dimensional island growth that generates voids between grains. Furthermore, the pristine SiO_2 surface has more interfacial trap states, which also hinder efficient charge transport. These explain the lowest field-effect mobility of the OFET without the SAM treatment. In the case of the DTS-treated OFET, the thin-film

https://doi.org/10.1021/acsomega.1c04519
ACS Omega 2021, 6, 33639−33644

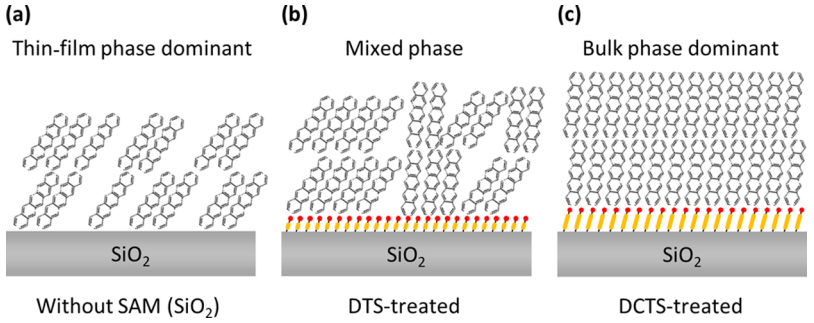

Figure 4. Schematic illustration of the crystalline phase of the pentacene films grown on (a) pristine, (b) DTS-treated, and (c) DCTS-treated SiO_2 surfaces.

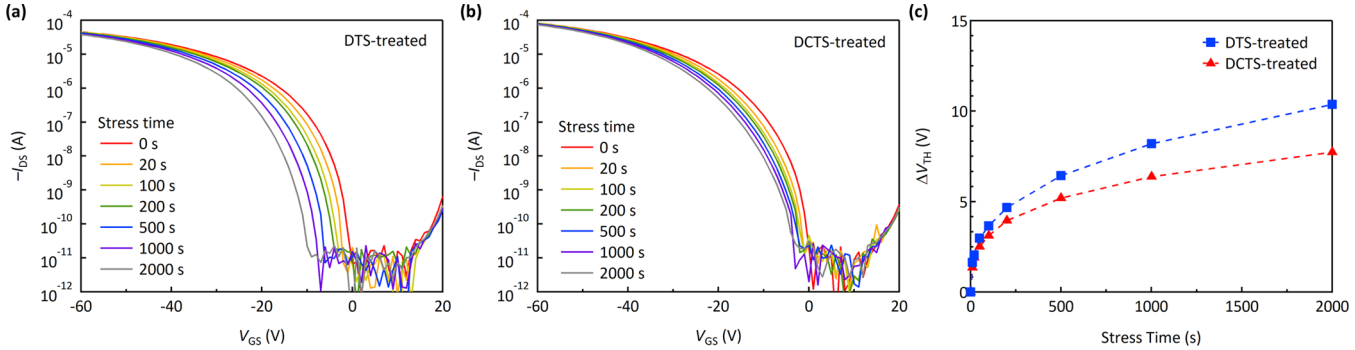

Figure 5. Evolution of the transfer characteristics of OFETs with (a) DTS treatment and (b) DCTS treatment under a gate bias stress of −60 V for 2000 s. (c) Threshold voltage shift of the OFETs with DTS and DCTS relative to stress time.

phase coexists with the bulk phase, as shown in Figure 4b. The mixture of these two phases generates structural defects and also disturbs the $\pi-\pi$ overlaps in the film, which, again, hinder efficient charge transport.[27,29] On the other hand, the pentacene film on DCTS exhibits a dominant bulk phase, which leads to the tight packing of pentacene molecules, as shown in Figure 4c. This results in an improved $\pi-\pi$ overlap of pentacene molecules and also reduces the number of structural voids in the film. These explain the 2-fold higher field-effect mobility of the DCTS-treated OFET relative to that of the DTS-treated OFETs.

Finally, we performed a gate bias stability test to determine if the differences in the electrical performances of DTS- and DCTS-treated OFETs can be attributed to the structural defects in the pentacene film on DTS, which arises from the coexistence of the two crystalline phases. The gate bias-induced instability in the OFETs is due to the charge trapping either at the semiconductor−gate dielectric interface or the bulk of the semiconductor. Because treatments with both SAMs have a similar passivating effect on the SiO_2 surface, differences in the gate bias-induced instability of the OFETs, if any, should be caused by the different defect densities in the pentacene films on DTS and DCTS. Figure 5a,b displays the evolution of the transfer characteristics of the OFETs with DTS and DCTS treatments, respectively, for 2000 s under a gate bias of −40 V. The transfer characteristics of the OFETs shift to the negative direction as mobile holes are trapped in the defect states by the applied gate bias, and consequently, the threshold voltages also change. Figure 5c shows the threshold voltage shift (ΔV_{TH}) of the OFETs with DTS and DCTS treatments with respect to the stress time. As shown in the figure, the OFET with the DTS treatment shows a larger threshold voltage shift during the test (10.4 V) than the OFET with the DCTS treatment (7.7 V) due to the large number of defect states arising from the coexistence of the two pentacene polymorphs, as described in Figure 4b. This also reaffirms that the mixed phase of the pentacene film on DTS has more structural defect states than the bulk-phase-dominant pentacene film on DCTS, which results in the inferior electrical performance of the DTS-treated OFETs relative to that of the DCTS-treated OFETs.

CONCLUSIONS

In summary, we examined the SAM-alkyl-chain-length-mediated crystalline phase of pentacene films and their effects on the electrical performance of pentacene-based OFETs. Two types of trichlorosilane SAMs, with alkyl chain lengths of 10 and 22 carbon atoms, were employed in this study, and both of them improved the morphology of pentacene by generating highly hydrophobic surfaces. Despite the similarities in the surface morphologies of pentacene grown on both the SAMs, the electrical performances of the OFETs vary significantly with the alkyl chain lengths of the SAM. To explain the differences in the electrical performances of the OFETs in terms of the SAM treatment they were subjected to, we investigated the crystalline phase of the pentacene films on SAMs with different alkyl chain lengths using XRD measurements. It was found that the pentacene film grown on the longer SAM (DCTS) exhibited dominant bulk-phase attributes while that on the shorter SAM (DTS) demonstrated the coexistence of the thin-film and bulk polymorphs. The mixed crystalline phase of pentacene yields structural defects in the film, which explains the SAM-alkyl-chain-length-dependent electrical performance of the OFETs. This study, therefore, provides new insights into the relationship between SAM properties and OFET performance and can therefore be used

https://doi.org/10.1021/acsomega.1c04519
ACS Omega 2021, 6, 33639−33644

to fully exploit the benefits of the SAM treatment in the field of organic electronics.

MATERIALS AND METHODS

Materials. DTS and DCTS were purchased from Sigma-Aldrich and Gelest, respectively. Pentacene was purchased from Tokyo Chemical Industry, and the solvents used in this work were purchased from Sigma-Aldrich. All materials were used as received without any purification.

Device Fabrication. Bottom-gate and top-contact pentacene-based OFETs were fabricated via thermal evaporation. In these devices, heavily doped silicon and thermally grown 300 nm SiO_2 films served as the gate and gate dielectric, respectively. The SiO_2 surface was treated with two types of trichlorosilane SAMs—DTS and DCTS—using a dipping method. A hexadecane solution containing 5 mM SAMs was prepared, and ultraviolet−ozone-treated SiO_2 substrates were dipped in the solution for 16 h. The substrates were then rinsed multiple times with isopropyl alcohol to remove the unreacted SAMs from the SiO_2 surface. This was followed by baking the substrates at 100 °C for 1 h on a hot plate to improve the uniformity of the SAM treatment and to remove any residual solvent. The SAM-treated substrates were then transferred to a vacuum chamber, where 60 nm pentacene and 50 nm Au films were thermally evaporated with shadow masks. The channel length (L) and width (W), defined by the shadow mask, were 40 and 1000 μm, respectively. To improve the morphology of the pentacene films, the substrates were held at 70 °C during the thermal evaporation process.

Characterization. The electrical performance of the pentacene-based OFETs was characterized using a semiconductor parameter analyzer (Agilent 4155C), and all electrical measurements were obtained in a nitrogen-filled glovebox. The capacitance of the 300 nm SiO_2 gate dielectric was measured to be 11.5 nF cm^{-2} and was found to be nearly unaffected by the SAM treatment. For the pentacene films, XRD measurements were conducted on the D8 Advance (Bruker Corp) platform using Cu Kα radiation (λ = 1.5406 Å) at 40 kV and 40 mA, while the AFM surface morphologies were characterized with the XE-100 microscope (Park System), operated in the noncontact mode.

ASSOCIATED CONTENT

Supporting Information

The Supporting Information is available free of charge at https://pubs.acs.org/doi/10.1021/acsomega.1c04519.

Summary of the previous studies examining the SAM-alkyl-chain-length-dependent mobility of pentacene-based FETs (PDF)

AUTHOR INFORMATION

Corresponding Author

Jeongkyun Roh − *Department of Electrical Engineering, Pusan National University, Busan 46241, Republic of Korea;* orcid.org/0000-0002-0674-572X; Email: jkroh@pusan.ac.kr

Authors

Myeongjin Park − *Department of Electrical and Computer Engineering, Inter-University Semiconductor Research Center, Seoul National University, Seoul 08826, Republic of Korea*

Chan-mo Kang − *Reality Display Research Section, Electronics and Telecommunications Research Institute, Daejeon 34129, Republic of Korea*

Sangwook Park − *Department of Electrical Engineering, Pusan National University, Busan 46241, Republic of Korea*

Hyeona Jo − *Department of Electrical Engineering, Pusan National University, Busan 46241, Republic of Korea*

Complete contact information is available at: https://pubs.acs.org/10.1021/acsomega.1c04519

Notes

The authors declare no competing financial interest.

ACKNOWLEDGMENTS

This work was supported by the National Research Foundation of Korea (NRF) grant funded by the Korean government (Ministry of Science and ICT) (nos. 2020R1C1C1013079 and 2021R1A4A1027087), Korea Institute for Advancement of Technology (KIAT) grant funded by the Korean Government (Ministry of Trade, Industry and Energy, MOTIE) (P0012451, The Competency Development Program for Industry Specialist), Materials/Parts Technology Development Program (20016195) funded by MOTIE, and 2020 BK21 FOUR Program of Pusan National University.

REFERENCES

(1) Mattana, G.; Loi, A.; Woytasik, M.; Barbaro, M.; Noël, V.; Piro, B. Inkjet-Printing: A New Fabrication Technology for Organic Transistors. *Adv. Mater. Technol.* **2017**, *2*, 1700063.

(2) Roh, J.; Kim, H.; Park, M.; Kwak, J.; Lee, C. Improved electron injection in all-solution-processed n-type organic field-effect transistors with an inkjet-printed ZnO electron injection layer. *Appl. Surf. Sci.* **2017**, *420*, 100−104.

(3) Ren, H.; Cui, N.; Tang, Q.; Tong, Y.; Zhao, X.; Liu, Y. High-Performance, Ultrathin, Ultraflexible Organic Thin-Film Transistor Array Via Solution Process. *Small* **2018**, *14*, 1801020.

(4) Shin, H.; Roh, J.; Song, J.; Roh, H.; Kang, C. M.; Lee, T.; Park, G.; An, K.; Kim, J. Y.; Kim, H.; Kwak, J.; Lee, C.; Kim, H. Highly Stable Organic Transistors on Paper Enabled by a Simple and Universal Surface Planarization Method. *Adv. Mater. Interfaces* **2019**, *6*, 1801731.

(5) Klauk, H.; Zschieschang, U.; Pflaum, J.; Halik, M. Ultralow-power organic complementary circuits. *Nature* **2007**, *445*, 745−748.

(6) Wang, C.; Zhang, X.; Dong, H.; Chen, X.; Hu, W. Challenges and Emerging Opportunities in High-Mobility and Low-Energy-Consumption Organic Field-Effect Transistors. *Adv. Energy Mater.* **2020**, *10*, 2000955.

(7) Paterson, A. F.; Singh, S.; Fallon, K. J.; Hodsden, T.; Han, Y.; Schroeder, B. C.; Bronstein, H.; Heeney, M.; McCulloch, I.; Anthopoulos, T. D. Recent Progress in High-Mobility Organic Transistors: A Reality Check. *Adv. Mater.* **2018**, *30*, 1801079.

(8) Yu, R.; Li, E.; Wu, X.; Yan, Y.; He, W.; He, L.; Chen, J.; Chen, H.; Guo, T. Electret-Based Organic Synaptic Transistor for Neuromorphic Computing. *ACS Appl. Mater. Interfaces* **2020**, *12*, 15446−15455.

(9) Ji, X.; Paulsen, B. D.; Chik, G. K. K.; Wu, R.; Yin, Y.; Chan, P. K. L.; Rivnay, J. Mimicking associative learning using an ion-trapping non-volatile synaptic organic electrochemical transistor. *Nat. Commun.* **2021**, *12*, 2480.

(10) Waldrip, M.; Jurchescu, O. D.; Gundlach, D. J.; Bittle, E. G. Contact Resistance in Organic Field-Effect Transistors: Conquering the Barrier. *Adv. Funct. Mater.* **2020**, *30*, 1904576.

(11) Park, S.; Kim, S. H.; Choi, H. H.; Kang, B.; Cho, K. Recent Advances in the Bias Stress Stability of Organic Transistors. *Adv. Funct. Mater.* **2020**, *30*, 1904590.

(12) Lashkov, I.; Krechan, K.; Ortstein, K.; Talnack, F.; Wang, S.-J.; Mannsfeld, S. C. B.; Kleemann, H.; Leo, K. Modulation Doping for Threshold Voltage Control in Organic Field-Effect Transistors. *ACS Appl. Mater. Interfaces* **2021**, *13*, 8664−8671.
(13) Sekitani, T.; Zschieschang, U.; Klauk, H.; Someya, T. Flexible organic transistors and circuits with extreme bending stability. *Nat. Mater.* **2010**, *9*, 1015−1022.
(14) Kim, S.-J.; Lee, J.-S. Flexible Organic Transistor Memory Devices. *Nano Lett.* **2010**, *10*, 2884−2890.
(15) Yuvaraja, S.; Nawaz, A.; Liu, Q.; Dubal, D.; Surya, S. G.; Salama, K. N.; Sonar, P. Organic field-effect transistor-based flexible sensors. *Chem. Soc. Rev.* **2020**, *49*, 3423−3460.
(16) Don Park, Y.; Lim, J. A.; Lee, H. S.; Cho, K. Interface engineering in organic transistors. *Mater. Today* **2007**, *10*, 46−54.
(17) Chen, H.; Zhang, W.; Li, M.; He, G.; Guo, X. Interface Engineering in Organic Field-Effect Transistors: Principles, Applications, and Perspectives. *Chem. Rev.* **2020**, *120*, 2879−2949.
(18) Shtein, M.; Mapel, J.; Benziger, J. B.; Forrest, S. R. Effects of film morphology and gate dielectric surface preparation on the electrical characteristics of organic-vapor-phase-deposited pentacene thin-film transistors. *Appl. Phys. Lett.* **2002**, *81*, 268−270.
(19) Miozzo, L.; Yassar, A.; Horowitz, G. Surface engineering for high performance organic electronic devices: the chemical approach. *J. Mater. Chem.* **2010**, *20*, 2513−2538.
(20) Pernstich, K. P.; Haas, S.; Oberhoff, D.; Goldmann, C.; Gundlach, D. J.; Batlogg, B.; Rashid, A. N.; Schitter, G. Threshold voltage shift in organic field effect transistors by dipole monolayers on the gate insulator. *J. Appl. Phys.* **2004**, *96*, 6431−6438.
(21) Hannah, S.; Cardona, J.; Lamprou, D. A.; Sutta, P.; Baran, P.; Al Ruzaiqi, A.; Johnston, K.; Gleskova, H. Interplay between Vacuum-Grown Monolayers of Alkylphosphonic Acids and the Performance of Organic Transistors Based on Dinaphtho[2,3-b:2′,3′-f]thieno[3,2-b]thiophene. *ACS Appl. Mater. Interfaces* **2016**, *8*, 25405−25414.
(22) Jang, S.; Son, D.; Hwang, S.; Kang, M.; Lee, S.-K.; Jeon, D.-Y.; Bae, S.; Lee, S. H.; Lee, D. S.; Kim, T.-W. Hybrid dielectrics composed of Al2O3 and phosphonic acid self-assembled monolayers for performance improvement in low voltage organic field effect transistors. *Nano Convergence* **2018**, *5*, 20.
(23) Hutchins, D. O.; Weidner, T.; Baio, J.; Polishak, B.; Acton, O.; Cernetic, N.; Ma, H.; Jen, A. K.-Y. Effects of self-assembled monolayer structural order, surface homogeneity and surface energy on pentacene morphology and thin film transistor device performance. *J. Mater. Chem. C* **2013**, *1*, 101−113.
(24) Roh, J.; Kang, C.-m.; Kwak, J.; Lee, C.; Jun Jung, B. Overcoming tradeoff between mobility and bias stability in organic field-effect transistors according to the self-assembled monolayer chain lengths. *Appl. Phys. Lett.* **2014**, *104*, 173301.
(25) Fukuda, K.; Hamamoto, T.; Yokota, T.; Sekitani, T.; Zschieschang, U.; Klauk, H.; Someya, T. Effects of the alkyl chain length in phosphonic acid self-assembled monolayer gate dielectrics on the performance and stability of low-voltage organic thin-film transistors. *Appl. Phys. Lett.* **2009**, *95*, 203301.
(26) Roh, J.; Lee, C.; Kwak, J.; Jung, B. J.; Kim, H. Vapor-phase-processed fluorinated self-assembled monolayer for organic thin-film transistors. *J. Korean Phys. Soc.* **2015**, *67*, 941−945.
(27) Dimitrakopoulos, C. D.; Brown, A. R.; Pomp, A. Molecular beam deposited thin films of pentacene for organic field effect transistor applications. *J. Appl. Phys.* **1996**, *80*, 2501−2508.
(28) Kang, S.-J.; Noh, Y.-Y.; Baeg, K.-J.; Ghim, J.; Park, J.-H.; Kim, D.-Y.; Kim, J. S.; Park, J. H.; Cho, K. Effect of rubbed polyimide layer on the field-effect mobility in pentacene thin-film transistors. *Appl. Phys. Lett.* **2008**, *92*, 052107.
(29) Kim, C.; Facchetti, A.; Marks, T. J. Gate Dielectric Microstructural Control of Pentacene Film Growth Mode and Field-Effect Transistor Performance. *Adv. Mater.* **2007**, *19*, 2561−2566.

https://doi.org/10.1021/acsomega.1c04519
ACS Omega 2021, 6, 33639−33644